Commensurate lock-in and incommensurate supersolid phases of hardcore bosons on anisotropic triangular lattices

Sergei V. Isakov,[1] Hong-Chi Chien,[2] Jian-Jheng Wu,[3] Yung-Chung Chen,[4] Chung-Hou Chung,[3] Krishnendu Sengupta,[5] and Yong Baek Kim[1]

[1]*Department of Physics, University of Toronto, Toronto, Ontario M5S 1A7, Canada*
[2]*Department of physics, National Tsing Hua University, Hsinchu, Taiwan 30013 R.O.C.*
[3]*Electrophysics Department, National Chiao Tung University, Hsinchu, Taiwan 300 R.O.C.*
[4]*Department of Physics, Tunghai University, Taichung, Taiwan 407 R.O.C.*
[5]*TCMP division, Saha Institute of Nuclear Physics, 1/AF Bidhannagar, Kolkata-700064, India*

(Dated: March 3, 2009)

We investigate the interplay between commensurate lock-in and incommensurate supersolid phases of the hardcore bosons at half-filling with anisotropic nearest-neighbor hopping and repulsive interactions on triangular lattice. We use numerical quantum and variational Monte Carlo as well as analytical Schwinger boson mean-field analysis to establish the ground states and phase diagram. It is shown that, for finite size systems, there exist a series of jumps between different supersolid phases as the anisotropy parameter is changed. The density ordering wavevectors are locked to commensurate values and jump between adjacent supersolids. In the thermodynamic limit, however, the magnitude of these jumps vanishes leading to a continuous set of novel incommensurate supersoild phases.

PACS numbers: 05.30.Jp, 67.40.-w, 75.40.Mg, 75.10.Jm

Introduction.— Supersolid phases with coexisting long-range diagonal and off-diagonal orders have long been recognized as interesting conceivable ground states of superfluid systems in the presence of mobile vacancies [1]. Recent experiments have also reported possible evidence for such a state in ^{4}He [2]. Another, relatively new, route to supersolid phases has recently been explored in the hardcore boson models on frustrated two-dimensional (2D) lattices [3, 4]. In such lattices, supersolid phases may arise due to intricate competition between kinetic and interaction energies, and as a result present an excellent playground for discovery of possible novel universality classes of quantum phase transitions [5, 6]. Further interest in these systems stems from potential realization of these models in ultracold atomic systems on optical lattices [7].

The diagonal (density) orders of the supersolid phases discovered so far have been restricted to commensurate orders. For example, a commensurate supersolid was discovered for the hardcore bosons on the isotropic triangular lattice [3] with the density ordering wave vector $\mathbf{Q}_0 = (4\pi/3, 0)$ along with non-vanishing superfluid order parameter [3]. A qualitative understanding of such a supersolid state can be obtained by considering the deviation from a commensurate boson filling fraction at which the ground state is a perfect Mott crystal with a long-range diagonal order. The additional particles or holes resulting from such a deviation condense to produce a superfluid while retaining the backbone of the existing Mott solid. This leads to the coexistence of off-diagonal (superfluid) and diagonal (Mott) orders. One may expect that incommensurate version of the supersolid phases may arise when there are more than one competing interactions or length scales in the system. If such a phase exists in lattice models, this may be a much closer analog of the supersolid phases originally proposed for the continuum.

In this letter, we investigate possible presence of incommensurate supersolid phases of the hardcore bosons at half-filling with anisotropic nearest-neighbor hopping and repulsive interactions on triangular lattices. We establish the ground states and phase diagram using several different and complementary methods, namely numerical quantum and variational Monte Carlo (QMC) techniques as well as analytical Schwinger-Boson mean-field theory. It is found that, for finite size systems, there exist a series of jumps between different supersolid phases as a function of the anisotropy parameter. The (density) ordering wavevectors of these phases are pinned to commensurate values and jump upon entering a nearby supersolid phase. The ordering wavevectors assume every single commensurate values for an interval of the anisotropy parameters. In the thermodynamic limit, however, we find that these ordering wavevectors become a continuous function of the anisotropy parameter, leading to a continuous set of incommensurate supersolids. We emphasize that such a continuous set of supersolid orders represent exciting discovery of novel quantum structures that have not been seen in previous studies of lattice boson systems.

Lattice Model.— We begin with the following hardcore boson model on an anisotropic triangular lattice.

$$H_{\rm b} = \sum_{\langle i,j\rangle} \left[-t_{ij}(b_i^\dagger b_j + \text{H.c.}) + V_{ij} n_i n_j \right] - \mu \sum_i n_i, \quad (1)$$

where b_i denotes the boson annihilation operator at site i and $\langle ij\rangle$ runs over the nearest-neighbor sites. The

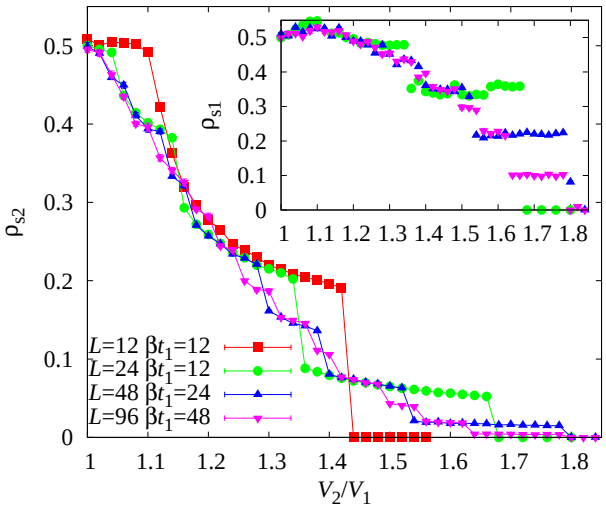

FIG. 1: The superfluid density along $\mathbf{a_2}$ as a function of the anisotropy parameter η for different system sizes and temperatures with $V_1/t_1 = 10$. The inset shows a similar plot for the superfluid density along $\mathbf{a_1}$. Lines are guides to the eye. The number of steps for $L = 12, 24, 48, 96$ are $3, 5, 9, 17$, respectively. The number of jumps between adjacent steps is hence $2, 4, 8, 16$, respectively.

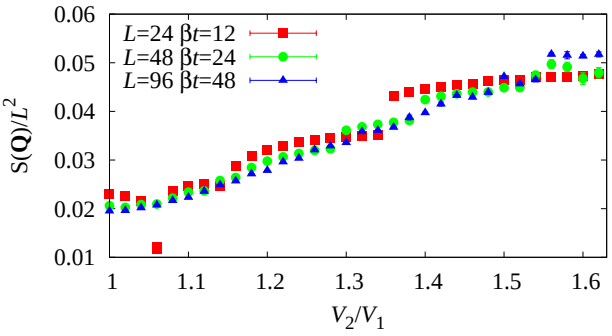

FIG. 2: The equal time structure factor $S(\mathbf{Q}(\eta))$ at the ordering wavevector $\mathbf{Q}(\eta)$ as a function of η for different system sizes and temperatures. All other parameters are the same as in Fig. 1. Judging from the size dependence of the data, the structure factor is clearly finite in the thermodynamic limit.

hopping t_{ij} and repulsive interaction V_{ij} are given by $t_{ij} = t_1(V_{ij} = V_1)$ and $t_{ij} = t_2(V_{ij} = V_2)$ for the nearest-neighbor sites along the diagonal and horizontal bonds of a triangular lattice (if it is viewed as a square lattice with one additional diagonal bond per each plaquette). Here we shall fix the anisotropy parameter $\eta = t_2/t_1 = V_2/V_1$. For $\eta = 1$, the model reduces to the well-known isotropic-triangular-lattice model. Such a hardcore boson model is also equivalent to an anisotropic spin-1/2 XXZ model via the well-known Holstein-Primakoff mapping [3].

In the isotropic case, the classical limit of this model ($t_{1,2} = 0$) has an extensive ground state degeneracy and power-law density-density correlations (or S_z-S_z correlator in the XXZ model) at zero temperature [8]. The ground state degeneracy at the isotropic point is completely lifted for $\eta < 1$ and the system orders at $\mathbf{Q}_1 = (\pi, \pi)$. On the contrary, the degeneracy is only partially lifted for $\eta > 1$. Here each diagonal chain is ordered antiferromagnetically at $\mathbf{Q}_2 = (\pi, 0)$ but the chains can be shifted with respect to each other giving rise to 2^L ground states, where L is the linear system size. We expect the first (second) type of ordering in the quantum model for $\eta \ll (\gg)1$ and call these phases solid I(II) for future reference. For the quantum model, when $t_{1,2}$ is turned on, it is well-known that the system exhibits a supersolid phase at $\eta = 1$ and large enough values of V_1/t_1 [3]. The key point which we want to address in this paper is the fate of the supersolid phase when $\eta \neq 1$.

Quantum Monte Carlo.— To address this problem, we perform QMC simulations using a plaquette generalization [9] of the Stochastic Series expansion (SSE) algorithm [10], where the elementary lattice unit is a triangle; this results in improved efficiency for large values of V_1/t_1. We measure the superfluid density along the diagonal ($\mathbf{a_2}$) and horizontal ($\mathbf{a_1}$) lattice directions by measuring the corresponding winding numbers $W^2_{\mathbf{a}_i}$ [11]: $\rho_{s1(2)} = W^2_{\mathbf{a}_{1(2)}}/\beta t_1$, where β is the inverse temperature. We also measure the equal time density-density correlator $S(\mathbf{q})/N = \langle \rho^\dagger_{\mathbf{q}\tau} \rho_{\mathbf{q}\tau} \rangle$, where $\rho_{\mathbf{q}\tau} = (1/N) \sum_i \rho_{i\tau} \exp(i\mathbf{q} \cdot \mathbf{r}_i)$ and $\rho_{i\tau}$ is the boson density at site i and imaginary time τ.

We begin with the case $\eta \geq 1$. A plot of the superfluid density ρ_{s2} along the $\mathbf{a}_2$ lattice direction is shown in Fig. 1 as function of η for different system sizes and temperatures. Notice that it exhibits a staircase structure with the number of steps proportional to the system size. Also, when the system size is doubled, the number of jumps between adjacent steps doubles and the gap between them decreases by half. The corresponding plot for ρ_{s1} is shown in the inset of Fig. 1. As can be clearly seen from both plots, the superfluid density undergoes several discontinuous jumps before reaching zero at $\eta \simeq 1.8$. Also, as shown in Fig. 2, the density-density correlator (in the thermodynamic limit) in each segment of η is finite at some ordering wavevector $Q(\eta)$ in the corresponding parameter range. Further, the ordering wavevector $\mathbf{Q}(\eta)$ is a constant along the "plateau" and changes discontinuously upon entering the next phase. Thus, for these finite size systems, the "plateaus" for $1 \leq \eta \leq 1.8$ correspond to distinct supersolid phases with sharp transitions between them.

Next we address the anisotropy dependence of the ordering wavevectors. The evolution of $\mathbf{Q} = (k_x, k_y)$ as a function of η is shown in Fig. 3. Here we have chosen $(k_x, k_y/\sqrt{3}) = (n_1\mathbf{b_1} + n_2\mathbf{b_2})/2\pi L$, where $\mathbf{b}_1 = 2\pi(1, 1/\sqrt{3}), \mathbf{b}_2 = 2\pi(0, 2/\sqrt{3})$ are the reciprocal lattice vectors and n_1, n_2 are integers. Comparing Fig. 3 and 1

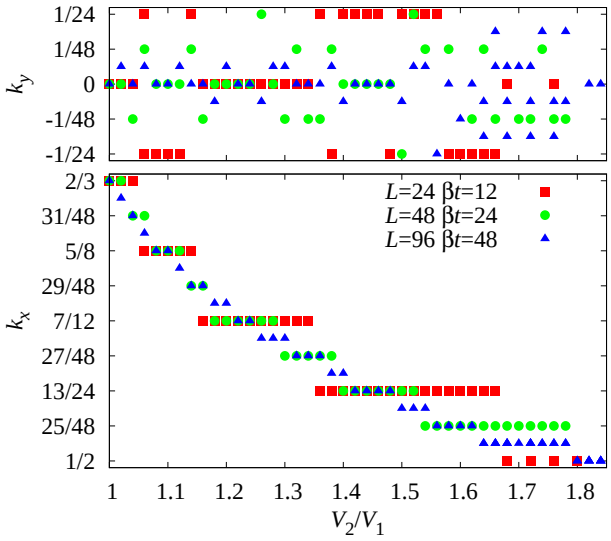

FIG. 3: The ordering wavevectors $\mathbf{Q}(\eta) = (k_x, k_y)$ as a function of η for different system sizes and temperatures. All the parameters are the same as in Fig. 1. Note that for odd $k_x L$, k_y cannot be zero and hence is off the axis. The data for $L = 96$ for $\eta > 1.6$ are not fully equilibrated, leading to the noisy behavior.

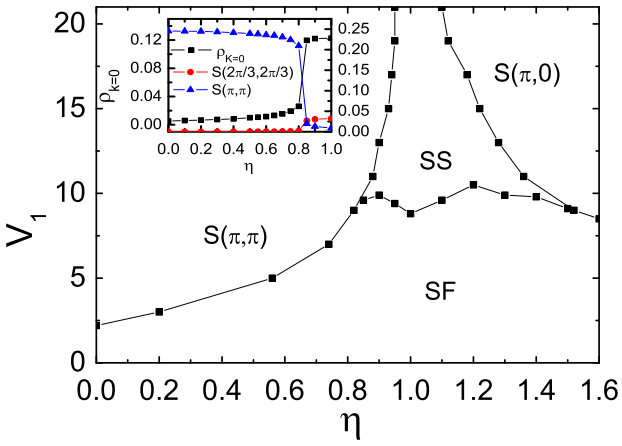

FIG. 4: Ground state phase diagram obtained by VMC as a function of η and V_1/t_1 for $L = 24$. The supersolid phase exists for $V_1 \geq 10t_1$ and between $0.8 \leq \eta \leq 1.5$. The inset shows the superfluid order parameter and the density-density correlators $S(\pi, \pi)$ and $S(2\pi/3, 2\pi/3)$ as a function of η for $V_1/t_1 = 9$. The transition from the Mott solid I to supersolid phase occurs at $\eta \simeq 0.8$.

we find that the system locks at rational wavevectors that are commensurate with the lattice in the "plateau" regions. The ordering wavevector goes from $\mathbf{Q}_0 = (4\pi/3, 0)$ at the isotropic point ($\eta = 1$) to $\mathbf{Q}_1 = (\pi, 0)$ at the transition point to the solid II phase ($\eta \simeq 1.8$), picking all possible commensurate values in between. The discontinuous jumps of $\mathbf{Q}(\eta)$ between these commensurate values decrease in magnitude with increasing system size. The nature of the phase diagram for $\eta < 1$, with $0.84 \leq \eta \leq 1$, turns out to be qualitatively similar. We again find a series of supersolid phase with the ordering wavevector pinned to commensurate values along the "plateaus", before the system reaches the Mott phase solid I at $\eta = 0.84$. The only difference comes from the fact that for $\eta < 1$, $k_x L$ is always even, so that k_y remains pinned to zero throughout the phase diagram.

Variational Monte Carlo.— We now supplement the QMC results with the VMC studies of the global phase diagram. Following Ref. [12], we use a variational wave function:

$$|\Psi\rangle = e^{-\frac{1}{2}\sum_{i,j} v_{i,j} n_i n_j} |\Phi_0\rangle, \qquad (2)$$

where $|\Phi_0\rangle = (b^\dagger_{k=0})^N |0\rangle$ is the non-interacting superfluid wave function and N is the total number of bosons. The components of the Jastrow potential, $v_{i,j} = v(|R_i - R_j|)$ are independently optimized to take into account the correlations between particles at different sites. The variational ground state energy decreases with larger number of $v_{i,j}$. For the present study, we have incorporated 15 $v_{i,j}$ parameters to make our result qualitatively and semi-quantitatively consistent with the QMC results. Standard Metropolis algorithm is used to calculate the variational energy. The method of statistical reconfiguration by Sorella [12] is employed to obtain the optimized parameters. With the optimized wave function, we compute the superfluid density $\rho(\mathbf{k}) = \sum_{i,j} e^{i(R_i - R_j)\cdot\mathbf{k}} \langle b^\dagger_i b_j \rangle$, the density-density correlator $S(\mathbf{q})$, and obtain the ground state phase diagram from these quantities[13].

The VMC results are summarized in Fig. 4 where the ground state phase diagram is shown as a function of η and V_1/t_1 for $L = 24$. Notice that a supersolid phase exists in the range $0.8 \leq \eta \leq 1.5$ for $V_1/t_1 \simeq 8$, which is qualitatively consistent with the QMC results. We have found that the upper limit of the phase boundary $\eta_u \simeq 1.5$ depends on the system size, and progresses towards larger values with increasing L. The lower phase boundary $\eta_l \simeq 0.8$ is virtually independent of the system size. For $\eta \leq \eta_l (\geq \eta_u)$, the system enters the Mott phase I(II) provided $V_1/t_1 \geq 8$. For weaker interactions, the superfluid phase prevails for all η. The inset of Fig. 4 shows the transition from the Mott I to the supersolid phase at $\eta \simeq 0.8$ for $L = 12$ and $V_1/t_1 = 9$. Note that the density-density correlator $S(2\pi/3, 2\pi/3)$ and the superfluid order parameter $\rho(\mathbf{k} = \mathbf{0})$ rise sharply while $S(\pi, \pi)$ drops to zero around this point, signifying a transition from the Mott I to the supersolid phase.

Schwinger Boson analysis.— Next, to obtain an analytical understanding of the η dependence of the ordering wavevector, and to determine the fate of the ordering wavevector plateaus in the thermodynamic limit, we

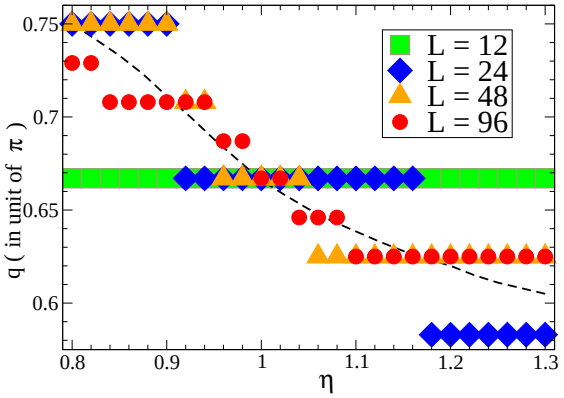

FIG. 5: (Color online) Plot of q (ordering wavevector is given by $\vec{Q} = (q, q)$) as a function of η for several finite system sizes (colored symbols) and in the thermodynamic limit (dashed line) as obtained from Schwinger boson mean-field analysis.

carry out a mean-field Schwinger boson analysis of Eq. 1. To this end, we start from the XXZ spin model description of Eq. 1 [3] and rewrite these spins in terms Schwinger bosons: $S_i^+ = a_i^\dagger c_i$ and $S_i^z = (a_i^\dagger a_i - c_i^\dagger c_i)/2$. Following standard procedure [14], we decouple the resultant Hamiltonian using the mean-field order parameters $A_\alpha = \langle a_i^\dagger a_{i+\alpha} + c_i^\dagger c_{i+\alpha}\rangle$ and $B_\alpha = \langle a_i c_{i+\alpha} - c_i a_{i+\alpha}\rangle$, where $\alpha = x, y$ for the horizontal/vertical and $\alpha = z$ for the diagonal bonds emanating from site i, to get the Schwinger boson mean-field free energy

$$f_{\rm MF} = \frac{A_x^2 + A_y^2 + A_z^2}{\eta(1 + V_1/t_1)} - \frac{B_x^2 + B_y^2 + B_z^2}{\eta(1 + V_1/t_1)} - (S + 1/2)\lambda - \frac{1}{N}\sum_{\mathbf{k}} A_{\mathbf{k}} + \frac{1}{2N}\sum_{\mathbf{k}} \omega_{\mathbf{k}}. \quad (3)$$

Here $A_{\mathbf{k}} = A_x \cos(k_x) + A_y \cos(k_y) + A_z \cos(k_x + k_y)$, $B_{\mathbf{k}} = B_x \sin(k_x) + B_y \sin(k_y) + B_z \sin(k_x + k_y)$, $\omega_{\mathbf{k}} = \sqrt{|\lambda - A_{\mathbf{k}}|^2 - B_{\mathbf{k}}^2}$ is the spinon dispersion, and the parameter λ is used to enforce the constraint of $2S = a_i^\dagger a_i + c_i^\dagger c_i$ at the mean-field level.

We obtain the values of mean-field variables at ground state by solving the saddle-point equations $\frac{\partial f_{MF}}{\partial A_\alpha} = \frac{\partial f_{MF}}{\partial B_\alpha} = \frac{\partial f_{MF}}{\partial \lambda} = 0$. The minima of the spinon dispersion $\omega(k)$ at $k_{min} = \pm(q/2, q/2)$ gives the spin order of the XXZ model with ordering wave-vector $\vec{Q} = (q, q)$ as shown in Fig. 5, both at finite sizes and in the thermodynamic limit. In the thermodynamic limit, for small $t_1/V_1 \simeq 0.04$, we find the supersolid phase for $0.8 \leq \eta \leq 1.3$ with *continually varying ordering wavevector* $\mathbf{Q}(\eta) = (q, q)$ as shown in Fig. 5. The corresponding spinon dispersion is gapless around both $\mathbf{k} = 0$ (which is a signature of superfluidity) and $\mathbf{k} = \pm(q/2, q/2)$ (which signifies the long-ranged solid order). For finite-size systems, we find that the spinon dispersion at $\mathbf{k} = \pm(q/2, q/2)$ acquires a gap which decreases with increasing system size and vanishes in the thermodynamic limit. Such a gap of the spinon dispersion leads to the staircase behavior of the ordering wave-vector as shown in Fig. 5. Our analytical Schwinger boson results are in qualitative agreement with both QMC and VMC results for finite system sizes and we therefore expect it to predict the correct behavior of the ordering wave-vector in the thermodynamic limit.

To conclude, we found that the hard-core boson system with competing interactions on anisotropic triangular lattices is locked to a series of commensurate supersolid phases for finite size systems, separated by series of jumps. This behavior is expected to occur, for example, in cold atom (bosons) systems on finite size optical lattices. In the thermodynamic limit, however, the ordering wavevector $\mathbf{Q}(\eta)$ becomes a continuous function of η, leading to a smooth crossover between a continuous set of novel incommensurate supersolids phases.

This work was supported by the NSERC, CIFAR, CRC, and KRF-2005-070-C00044 (SV and YBK); NSC 95-2112-M-009-049-MY3 (JJW and CHC) and NSC 96-2112-M-029-003-MY3 (HCC and YCC) via the MOE ATU Program of Taiwan. Some of the numerical works was supported by the National Center of High Performance Calculation and the NCTS of Taiwan. We also thank Roderich Moessner for helpful discussions.

[1] O. Penrose and L. Onsager, Phys. Rev. **104**, 576 (1956); A. F. Andreev and L. M. Lifschitz, Zh. Eksp. Teor. Fiz. **56**, 2057 (1969) [Sov. Phys. JETP **29**, 1107 (1969)]; A. J. Leggett, Phys. Rev. Lett. **25**, 1543 (1970).
[2] E. Kim and M.H.W. Chan Nature **427**, 225 (2004).
[3] G. Murthy, D. Arovas, and A. Auerbach, Phys. Rev. B **55**, 3104 (1997); S. Wessel and M. Troyer, Phys. Rev. Lett. **95**, 127205 (2005); D. Heidarian and K. Damle, Phys. Rev. Lett. **95**, 127206 (2005); R. G. Melko *et al*, Phys. Rev. Lett. **95**, 127207 (2005); M. Boninsegni and N. Prokof'ev, Phys. Rev. Lett. **95**, 237204 (2005).
[4] G.G. Batrouni *et al.*, Phys. Rev. Lett. **74**, 2527 (1995), P. Sengupta *et al.*, Phys. Rev. Lett. **94**, 207202 (2005), S. Wessel, Phys. Rev. B **75**, 174301 (2007).
[5] L. Balents *et al.*, Phys. Rev. B **71**, 144508 (2005); A. A. Burkov and L. Balents, Phys. Rev. B **72**, 134502 (2005).
[6] S. V. Isakov *et al.*, Phys. Rev. Lett. **97**, 147202 (2006); K. Sengupta, S. V. Isakov and Y. B. Kim Phys. Rev. B **73**, 245103 (2006).
[7] M. Greiner *et al.*, Nature **415**, 39 (2002); A. Griesmaier *et al.*, Phys. Rev. Lett. **94**, 160401 (2005).
[8] G. H. Wannier, Phys. Rev. **79**, 357 (1950); R. M. F. Houtappel, Physica **16**, 425 (1950); J. Stephenson, J. Math. Phys. **11**, 413 (1970).
[9] K. Louis and C. Gros, Phys. Rev. B **70**, 100410(R) (2004).
[10] A. W. Sandvik, Phys. Rev. B **59**, R14157 (1999); O. F. Syljuåsen and A. W. Sandvik, Phys. Rev. E **66**, 046701 (2002).
[11] E. L. Pollock and D. M. Ceperley, Phys. Rev. B **36**, 8343 (1987).

[12] M. Capello, F. Becca, M. Fabrizio, and S. Sorella, cond-mat/0611306; S. Sorella, Phys. Rev. B **71**, 241103(R) (2005).

[13] Note that we have fitted the Jastrow potential v(R) in the form of power-law function: $v(R) \sim 1/R^c + constant$ ($c \sim 1$), which is consistent with the previous calculation (see, for example N. Trivedi and D.M. Ceperley, Phys. Rev. B 40, 2737 (1989)) . We find slight deviation from 1/R decay at small system sizes due to the finite-size effect.

[14] C. J. De Leone and G. T. Zimanyi Phys. Rev. B **49**, 1131 (1994).